

Article

Substantiation of the Effectiveness of Water-Soluble Hydrophobic Agents on the Properties of Cement Composites

Jakub Hodul *, Tatiana Beníková and Rostislav Drochytka 

Faculty of Civil Engineering, Brno University of Technology, 602 00 Brno, Czech Republic; tatiana.benikova@vut.cz (T.B.); rostislav.drochytka@vut.cz (R.D.)

* Correspondence: jakub.hodul@vut.cz

Abstract: This paper aims to verify the effect of water-soluble hydrophobisations on cementitious composites such as concrete (S1) and cement-bonded particle boards (S2). The research was focused on the water-soluble hydrophobisations based on methylsilanolate (MS), a mixture of silanes and siloxanes (SS) and alcohol with the addition of nano-silica (N). The results provide a comprehensive overview of the benefits and effectiveness of water-soluble hydrophobisations in the context of building materials, outlining a direction towards the development of new, more environmentally friendly solutions in the construction industry. For this reason, alternative raw materials (brick recyclate and brick dust) were used for S1 substrate preparations. How the water-soluble hydrophobisations, including hydrophobisations with the addition of nano-silica (N), affect the process of water evaporation during hydration and the resulting water repellence of the S1 and S2 substrates were experimentally verified through a series of tests, e.g., measurement of the contact angle and depth of water penetration under pressure. The evaluation of the effect of hydrophobisations on the resistance of substrate to aggressive gaseous and liquid environments was observed by the determination of the resistance to carbonation and sulphation processes and the resistance of the concrete to aggressive liquid media (10% H₂SO₄, 10% CH₃COOH). Although the hydrophobisations did not have a significant effect on some aspects of S1, such as the resistance to carbonation and sulphate attack, improvement was observed in other areas, such as the quadrupling increase in contact angle of the surface and 9 mm decrease in water pressure penetration into the concrete substrate.

Keywords: water-soluble hydrophobic agent; durability; concrete; cement-bonded particle board; contact angle; chemical resistance



Citation: Hodul, J.; Beníková, T.; Drochytka, R. Substantiation of the Effectiveness of Water-Soluble Hydrophobic Agents on the Properties of Cement Composites. *Buildings* **2024**, *14*, 3364. <https://doi.org/10.3390/buildings14113364>

Academic Editor: Yun Gao

Received: 29 July 2024

Revised: 13 October 2024

Accepted: 16 October 2024

Published: 24 October 2024



Copyright: © 2024 by the authors. Licensee MDPI, Basel, Switzerland. This article is an open access article distributed under the terms and conditions of the Creative Commons Attribution (CC BY) license (<https://creativecommons.org/licenses/by/4.0/>).

1. Introduction

Hydrophobic impregnations, as an important part of surface protection, play an important role in increasing the resistance of cementitious composites to water and other aggressive substances, such as chlorides and sulphates. This resistance is a critical factor for improving the durability and sustainability of structures, as underlined by several studies [1–3]. Recent decades have shown a clear trend in the use of hydrophobic impregnations, not only in industrial and residential buildings but also in infrastructural and historical buildings, which shows their widespread application [4,5]. Modern approaches to the development of hydrophobic impregnations, including those with the addition of nanoparticles, e.g., silver, ZnO or SiO₂, also promise to improve the durability of cementitious composites containing alternative raw materials, which are increasingly used in current construction practice [6,7].

An analysis by studies [8–10] reveals that most of the hydrophobising products are silane- or siloxane-based, often diluted with water, indicating the increasing trend of the use of water-soluble hydrophobisations. This approach suggests a trend towards water-soluble hydrophobisations, which are more environmentally preferable due to the absence of volatile organics, such as xylene, hexane, etc., from diluents and can serve as a basis for

further research towards the development of more durable, environmentally acceptable hydrophobisation systems.

Hydrophobic impregnations give cementitious composites a water repellent effect by increasing the contact angle of water droplets and reducing the surface energy of the material, allowing water to run off the surface more efficiently and minimising the formation of wet areas. The impregnations penetrate the pore structure where they react with the substrate to form a hydrophobic layer [11]. The primary mechanism of this process is the reaction of the molecular functional groups of these substances with the hydroxyl groups on the surface of cementitious materials. Unlike typical coatings, the hydrophobised material is porous and does not block the original structure, allowing water vapor to exchange with the outside environment [12,13]. Current studies show that hydrophobic impregnations should not significantly affect the air and water vapor permeability of the material, which is key to maintaining the necessary gas exchange and water vapor permeability [14,15]. The results of Zhang et al. [16] and Herb et al. [17] suggest that hydrophobic silane- and siloxane-based products do not typically prevent CO₂ penetration but may reduce their permeability to CO₂ under certain conditions (the concentration of CO₂ gas was maintained constant at $20 \pm 2\%$; relative humidity 70%; the temperature was 20 ± 3 °C). According to Wu et al. [18], the lack of permeability to water vapor can cause significant damage during freezing and thawing due to the accumulation of water beneath the surface, which negatively affects the durability of cementitious composites [19,20].

Like in the relevant literature [21–23], the basic properties of hydrophobic impregnations, including penetration depth and contact angle, were tested in this research. Penetration depth provides critical data on the ability of hydrophobic agents to penetrate deeply into the microstructure of a material to provide effective protection [24]. The contact angle, on the other hand, reflects changes in the hydrophobic properties of the surface, which manifests itself in increased resistance to water absorption. These properties are essential for an objective evaluation of the effectiveness of hydrophobic impregnations [25]. The durability of reinforced concrete structures in marine environments, regardless of binder type, can effectively be improved using silane hydrophobic impregnation, assuming proper concrete surface preparation and application methods [26].

This paper focuses on the detailed verification of commercially available water-soluble hydrophobic impregnations and their effect on the properties of cementitious composites, e.g., water repellence of the surface, resistance to carbonation and sulphate resistance, penetration of water under pressure, etc. The aim is not only to analyse their hydrophobic properties but also to investigate the possibilities of their application in a broader context, such as use in a chemically aggressive environment and in places where pressurised water is used. It also considers current trends in the production of cementitious composites and the environmental factors associated with their production. The correct application of water-soluble hydrophobic impregnation can significantly extend the durability of cementitious composites and improve the properties of cementitious composites made from alternative raw materials. Secondary raw materials are increasingly being used in the cement industry, but this also raises a number of challenges that need to be overcome, such as the long-term durability and stability of concrete composition. Water-soluble hydrophobic impregnations can help mitigate these challenges, contributing to the overall performance and sustainability of concrete and cement-bonded particle boards containing by-products. This study is innovative for various reasons, mainly in using new water-soluble hydrophobic agents on the concrete (S1) and cement-bonded particle board (S2) substrates and monitoring the resistance of hydrophobised concrete to carbonation, sulfation and aggressive liquid environments.

2. Materials and Methods

2.1. Hydrophobic Agents and Substrate

In the research, three types of commercially available hydrophobic impregnations are used. The first hydrophobic impregnation is based on methylsilanolate (MS). The

second hydrophobic impregnation is a mixture of silanes and siloxanes (SS). The third hydrophobic impregnation used is alcohol with added nano-silica (N). MS (Lukofob 39, manufactured by Lucerne závody, a.s, Kolín, Czech Republic) hydrophobic impregnation is engineered to improve porous light-coloured silicate materials' resistance to water. This product is significant for its cost-effectiveness and minimisation of environmental impact. Its application is flexible, allowing for different application methods depending on the required degree of dilution of the concentrate with water, which ranges from 1:10 to 1:100. This variability allows the application process to be optimised by coating, spraying or dipping, adapted to specific requirements. The protective hydrophobic SS impregnation (PCI Silconal® W, manufactured by Master Builders Solutions CZ s.r.o., Chrudim, Czech Republic) is intended for the impregnation of facades, building parts or chimneys. It is also suitable for the hydrophobisation of monuments made of sandstone, natural materials or solid brick. This product is exceptional because of its solvent-free composition, which allows for its application in both outdoor and indoor environments. This hydrophobic impregnation is supplied in a form that requires no dilution, making the application process simpler. Nano-impregnation N (NanoConcept®, manufactured by IMPRE CZ s.r.o, Brno, Czech Republic) is chosen for its effectiveness in improving concrete, brick and other materials with excellent water repellence, antibacterial properties and self-cleaning ability. This product is suitable for application in both outdoor and indoor environments, without the need for dilution, which makes it easy to apply. Suitable application methods are spraying or coating.

The selected water-soluble hydrophobisations are commercially available, and suitable for the purpose of soaking samples. Their long-term durability in an aggressive environment has not yet been investigated, and neither has their effect on improving the properties of concrete containing brick recycle and cement-bonded particle boards. The hydrophobic impregnations have different dilution needs before application, as well as different colours and pH values. However, all hydrophobic impregnations are supplied in a liquid form and are low-viscosity and low-volume due to the values declared by the manufacturers in the data sheets of the hydrophobic impregnations. The basic physical properties of the water-soluble hydrophobisations used are shown in Table 1.

Table 1. Selected properties of the hydrophobic impregnations [27–29].

Parameter	MS	SS	N
Component ¹ [-]	2	1	1
Colour [-]	Transparent to yellowish	White	Orange, yellow
Consumption ² [L/m ²]	0.5–1.0	0.25–0.4	0.1–0.2
Density [g/cm ³]	1.27–1.3	1	1.058
pH value [-]	13–14	6	4

¹ A value of 1 indicates the use of hydrophobisation without additional dilution; a value of 2 indicates the use of hydrophobisation after dilution with water. ² Consumption ranges depend on the substrate being used (S1 was more absorbent).

The hydrophobic impregnations were applied to two different types of cement composites. The first type (substrate S1) was a cementitious composite with brick recycle, composed of CEM II/B-M cement (S-LL) 32.5 R (Českomoravský cement, a.s., Mokrý, Czech Republic), fine quarried aggregate fraction 0–2 mm (Žabčice, Czech Republic), coarse crushed aggregate fraction 4–8 mm (Žabčice, Czech Republic), coarse crushed aggregate fraction 8–16 mm (Olbramovice, Czech Republic), brick recycle fraction 0–1 mm and 0–4 mm (Wienerberger s.r.o., Šlapanice, Czech Republic) and a polycarboxylate-based superplasticising admixture STACHEMENT 6358 FM (STACHEMA CZ s.r.o., Kolín, Czech Republic) with a water coefficient of 0.6. Used brick dust is waste from brick formatting taken directly from brick production. Recycled brick was made from waste bricks and crushed to a fraction of 0–4 mm under laboratory conditions. The composition of cement composite S1 per 1 m³ is stated in Table 2. Substrate S2 was represented by cement-bonded particle boards by CETRIS®BASIC with a smooth cement-grey surface of 22 mm thickness,

manufactured by CIDEM Hranice a.s. (Hranice, Czech Republic), with a 5% replacement of cement (CEM I 42.5 R) by limestone. The properties of S2 are stated in Table 3.

Table 2. Composition of the cement composite (substrate S1) per 1 m³.

Component	Unit	Amount for 1 m ³
CEM II/B-M (S-LL) 32.5 R	[kg]	300
Fine aggregate 0/2	[kg]	661
Coarse aggregate 4/8	[kg]	266
Coarse aggregate 8/16	[kg]	570
Brick recycle 0/4	[kg]	117
Brick dust 0/1	[kg]	117
Water	[l]	190
Polycarboxylate-based superplasticiser	[kg]	3.3

Table 3. Basic properties of the cement-bonded particle boards (substrate S2) [30].

Parameter	Average Real Values
Density	1350–1500 kg/m ³
Flexural strength	min. 11.5 N/mm ²
Modulus of elasticity	min. 6800 N/mm ²
Water absorption *	max. 16%
Freeze–thaw resistance **	R _L = 0.97
pH	12.5
Resistance of surface to water and defrosting chemicals ***	loss max. 20.4 g/m ²

* Water absorption of the slab when immersed in water for 24 h. ** Freeze–thaw resistance at 100 cycles according to EN 1328 [31]. *** Surface resistance to the effects of water and chemical de-icing agents according to ČSN 73 1326 [32], loss after 100 cycles by Method A.

Due to the low viscosity of hydrophobic impregnations, the samples were prepared using a method where the substrate was immersed in the hydrophobic impregnation solution. The application process of the hydrophobic impregnation can be seen in Figure 1. The hydrophobicity treatments were applied to all substrate types 24 h after the specimens' creation to limit evaporation of the water. Prior to application, the cementitious composites were cleaned; dust and minor impurities were removed mechanically with a steel spatula. Sample soaking was performed under standard laboratory conditions at 21 °C. The samples were dipped in the hydrophobic impregnation on each side to ensure that it was applied to their entire surface. All substrates were immersed in the hydrophobisation for approximately one minute on each side. In cases where the substrates were not well wetted by the hydrophobisation after visual inspection, they were left in the container of hydrophobisation until the entire surface was wetted. After the impregnation was completed, the specimens were gently removed from the hydrophobicity and left in an inclined position. The specimens were then placed on grids where drying was carried out under laboratory conditions. The specimens were afterwards left under laboratory conditions for 28 days.

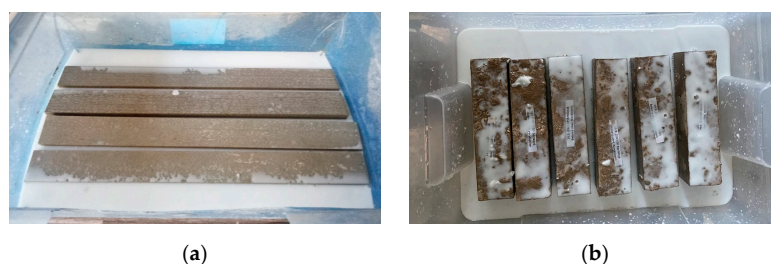


Figure 1. Application of SS hydrophobic impregnation on the cement composite surface by soaking: (a) substrate S2 (rectangular prism, dimensions 50 × 500 × 22 mm), (b) concrete substrate S1 (prism, dimensions 40 × 40 × 160 mm) with remains of the hydrophobisation on the surface.

2.2. Experimental Methods

2.2.1. Dynamic Viscosity

Prior to the application of the hydrophobic impregnations, the dynamic viscosity was determined using a ViscoQC 300H rotational viscometer (Anton Paar GmbH, Graz, Austria); see Figure 2. The viscosity measurement of the hydrophobic impregnation was performed according to the EN ISO 2884-2 standard [33]. The viscosity measurement was performed at a constant temperature of 20 °C. From the set of available spindles, the RH2 spindle was used because it was expected that the measured hydrophobic impregnations would have low viscosity. The dynamic viscosity was read at the maximum speed of 250 revolutions per minute at the maximum torque, after 2 min from the start of the measurement.



Figure 2. Determination of the dynamic viscosity of SS hydrophobisation.

2.2.2. Penetration Depth

The penetration depth of the hydrophobic impregnation was determined using a KEYENCE VHX 750F digital microscope (Keyence Ltd., Osaka, Japan). At real magnification 64×, the penetration depth was measured several times at different locations on the cut surface. Measurements were performed on 28-day-old prism specimens measuring 40 × 40 × 160 mm using Keyence communication software ver. 3.0 for VHX 950F. To better determine the penetration depth of the hydrophobic impregnations, a small amount of red liquid pigment concentrate was added to each hydrophobic impregnation before they were applied to the substrates.

2.2.3. Determination of Surface Wettability

Static measurements of the contact angle and surface energy were performed using the surface energy evaluation system (See System) and a charge-coupled device (CCD) camera (produced by Faculty of Mechanical Engineering BUT, Brno, Czech Republic).

A measured drop of liquid was applied to the surface of the hydrophobised surfaces of the test specimens. Three types of selected liquids were used, namely water, glycerol and ethylene glycol. The measurement was then carried out on the See System device using a CCD camera (Figure 3), which captured an image of the sample. The image captures the three-phase interface of solid, liquid and gas, as well as the boundary between the sessile droplet and the surrounding gaseous environment. With the help of these obtained data, the individual tangents at the phase interface are then determined and the contact angle between the liquid and the solid is subsequently obtained. Finally, the combination of the acid–base (Lifshitz–Van der Waals) method and the Young–Dupr’e equation determines

the surface energy and its components. The dispersion of the wetting angle is due to the fact that its value was determined on samples of five drops.



Figure 3. CCD camera for measuring the contact angle and surface energy of the hydrophobised surface.

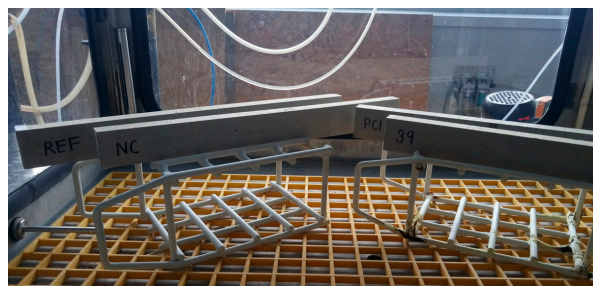
2.2.4. Chemical Resistance to Aggressive Environment

To study the effect of hydrophobisations on the carbonation and sulphation processes, prisms measuring $40 \times 40 \times 160$ mm 14 days after the application of hydrophobisation were placed in corrosion gas chambers where they were exposed to the gases SO_2 and CO_2 . The specimens were placed in an HCP 108 climate chamber (Memmert GmbH + Co.KG, Schwabach, Germany) to expose them to a CO_2 concentration of 10% at a temperature of 25°C and a relative humidity of 50% for 40 days without interruption. The resistance to exposure to a moist atmosphere containing SO_2 was tested according to EN ISO 22479 [34]. Further samples were placed in an HK 800 corrosion gas chamber (Köhler Automobiltechnik GmbH, Lippstadt, Germany) and exposed to an environment with 3.375% SO_2 concentration. In the first 1.5 h, the temperature in the chamber was raised to $40 \pm 3^\circ\text{C}$ and maintained at this temperature for the next 6.5 h. At the end of the eight-hour cycle, the heating was turned off and the chamber door was opened for 16 h under laboratory conditions. The specimens were exposed to 40 cycles.

Based on the need to evaluate the effect of the application of hydrophobic impregnation on the resistance of the material to acidic solutions, the specimens were placed in a 10% sulphuric acid or 10% acetic acid solution (Figure 4a). The samples of S1 with dimensions $40 \times 40 \times 160$ mm, S2 samples with dimensions $50 \times 50 \times 25$ mm impregnated by the hydrophobisations, and untreated reference samples were tested. Samples were placed in sulphuric and acetic acid solutions 28 days after the application of hydrophobisation and left in this acidic environment for 14 days.



(a)



(b)

Figure 4. Samples treated with hydrophobic impregnations in the aggressive chemical environments: (a) substrate S1 in sulphuric and acetic acid solutions; (b) substrate S2 in a moist atmosphere containing SO_2 .

First, the microstructure of S1 samples exposed to aggressive gaseous and liquid environments was studied. This was performed using a KEYENCE VHX 750F digital microscope (Keyence Ltd., Osaka, Japan) at $64\times$ magnification and a TESCAN MIRA3 XMU scanning electron microscope (SEM) with 3D imaging capability (TESCAN, Brno, Czech Republic). The idea was to monitor changes caused by carbonation or sulphation at the microscopic level. In order to determine the microstructure using SEM, samples with an area of approximately 2 cm^2 and a thickness of 3 mm were taken from the surface of the hydrophobised substrate, which was exposed to the aggressive environment (SO_2 , CO_2). All MIRA chambers can be used to conveniently place samples in a 5-axis motorised sample table. It is also equipped with SE, BSE, CL and LVSTD detectors for working under high and low vacuum and is supplemented with a Bruker EDX analyser for determining the elemental composition. Samples were coated with a layer of gold for this observation, using the SEM in low-vacuum mode and an accelerating voltage of 20 kV.

Second, the degree of carbonation and sulphation of the samples after exposure in an aggressive gaseous or liquid environment was evaluated using a solution of 1% phenolphthalein, ethyl alcohol and water. The samples were fractured, and the fracture surfaces were sprayed with phenolphthalein solution. The surfaces which turned purple had a pH higher than 9.0. The depth of carbonation, which is the area from the purple colouration to the edge of the sample, was then measured several times on each sample. To verify the carbonation and sulphation degree of the samples exposed to an aggressive environment, the amount of carbonation and sulphation products was detected by diffraction thermal analysis. The analysis was carried out on reference specimens of S1 and an S2 specimen treated with hydrophobic N impregnation. These specimens were exposed to the aggressive gaseous environment of SO_2 (Figure 4b) and CO_2 . The samples were 60 days old and crushed to dust before testing. A Mettler Toledo TGA/DSC 1 instrument (Mettler-Toledo, LLC, Columbus, OH, USA) was used for the differential thermal analysis [35]. The samples exposed to the CO_2 atmosphere were subsequently subjected to differential thermal analysis (DTA) in order to determine the carbonation products and the effect of individual hydrophobisation on the resistance of concrete to carbonation. Samples were taken approximately 1 cm from the surface and ground to a particle size below 0.063 mm. The samples were then heated in a DTA analyser to a temperature of $1100\text{ }^\circ\text{C}$.

2.2.5. Depth of Penetration of Water Under Pressure

Depth of penetration of water under pressure was performed according to the standard EN 12390-8 [36]. Specimens were cube-shaped with dimensions of $150 \times 150 \times 150\text{ mm}$ and were exposed to water pressure of $500 \pm 50\text{ kPa}$ (Figure 5). After $72 \pm 2\text{ h}$, specimens were fractured vertically to the surface of the applied pressure, then the depth of penetration was measured.



Figure 5. S1 samples treated by the hydrophobisation in the apparatus for the determination of the depth of penetration of water under pressure.

2.2.6. Shrinkage

The shrinkage of the S1 concrete mix was monitored using prism-shaped troughs with a length of 250 mm, a width of 80 mm and a height of 60 mm; see Figure 6. The trough was constructed from three fixed walls, a floor and one movable wall. Before filling the material, the whole assembly was padded with a slippery material (neoprene) and covered by a plastic separating layer. This setup assured the free movement of material inside the troughs. To control the direction of shrinkage and make the measurements possible, two anchors were fixed to the assembly, first to the movable segments and second to the opposite fixed wall. The deflectometer threw extension measures of the movable parts, and the relative length changes were recorded in micrometres. The volume changes were monitored at regular time intervals and the data were recorded.

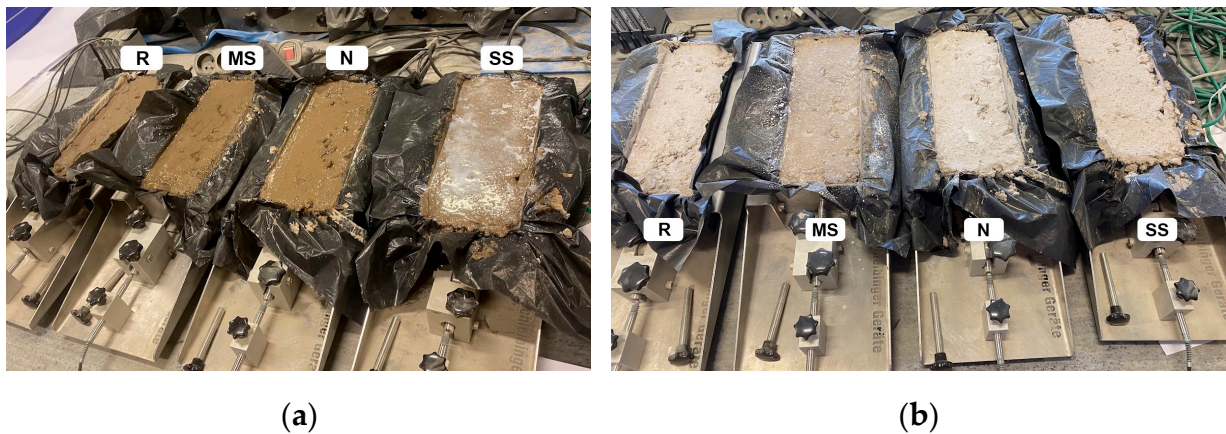


Figure 6. Measurement of shrinkage of S1 mixtures treated with hydrophobic impregnations in the troughs: (a) after the application of hydrophobic impregnation; (b) at the end of the measurements—after 28 days.

Four troughs were filled with the S1 concrete mix immediately after mixing. The concrete mix in the troughs was compacted and, approximately two hours after compaction, a layer of hydrophobic impregnation, MS, SS or N, was sprayed onto the surface of the three samples. The measurement process continued for 28 days, during which the shrinkage in $\mu\text{m}/0.25\text{ m}$ was recorded. The values were multiplied by four to show the results in $\mu\text{m}/\text{m}$, providing a standardised measurement of shrinkage per metre. The tested samples filled with S1 concrete mix after the application of the hydrophobic spray impregnation are shown in Figure 6a, and the tested samples at the end of the measurements after 28 days are shown in Figure 6b.

2.2.7. UV Resistance

The resistance of the samples treated by the water-soluble hydrophobic impregnations to ultraviolet (UV) was monitored using a xenon system for accelerated aging of materials by artificial sunlight—Q-SUN XE3HS (Q-Lab, Westlake, OH, USA), according to EN ISO 4892-2 Part 2: Xenon lamps. Method A cycle 1 [37]. The chamber with hydrophobised samples that reproduce the damage caused by full-spectrum sunlight and rain can be seen in Figure 7. The parameters of the Q-SUN chamber to which the experimental samples were exposed are shown in Table 4.

The S2 samples were alternately exposed to UV radiation, heating and water scraping. The samples were exposed to these conditions for 840 h. The aim of this test was to simulate the different climatic conditions to which hydrophobic impregnations may be exposed under real weather conditions. Visual changes of the sample surfaces were monitored at regular intervals every 84 cycles.

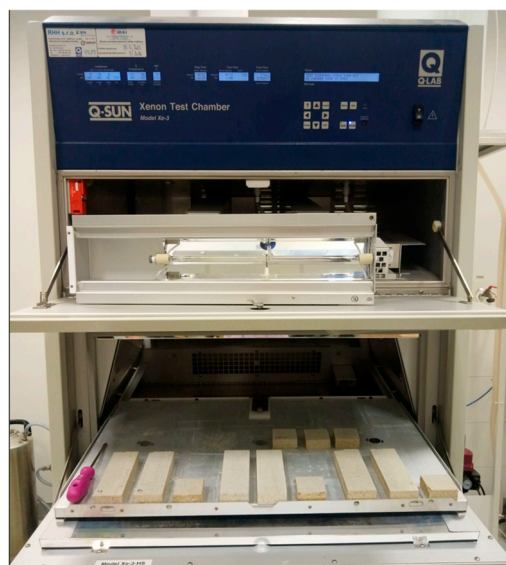


Figure 7. Samples in the full-featured lightfastness, colourfastness, and photostability chamber Q-SUN Xe-3 tester.

Table 4. Q-SUN chamber parameters of the simulated environment to which the reference samples and samples treated with hydrophobisation on the substrate S2 were exposed.

Parameter	Value	Unit
Temperature of chamber	38 ± 3	$^{\circ}\text{C}$
Relative humidity	50 ± 10	%
Short-wavelength irradiance (300–400 nm)	60 ± 2	W/m^2
Long-wavelength irradiance (<400 nm)	0.51 ± 0.02	MJ/m^2

3. Results and Discussion

3.1. Dynamic Viscosity

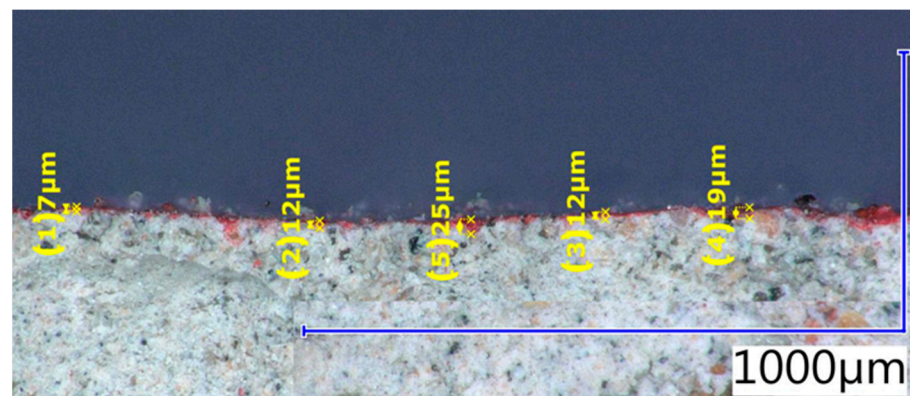
The measured values of dynamic viscosity of the hydrophobisations are seen in Table 5. The dynamic viscosity of the MS hydrophobic impregnation is approximately two times greater than that of the other two products used. For this reason, the MS impregnation was diluted with additional water at a ratio of 1:0.7 before use. The hydrophobic N and SS impregnations were not diluted before application.

Table 5. Dynamic viscosity of the hydrophobic impregnations.

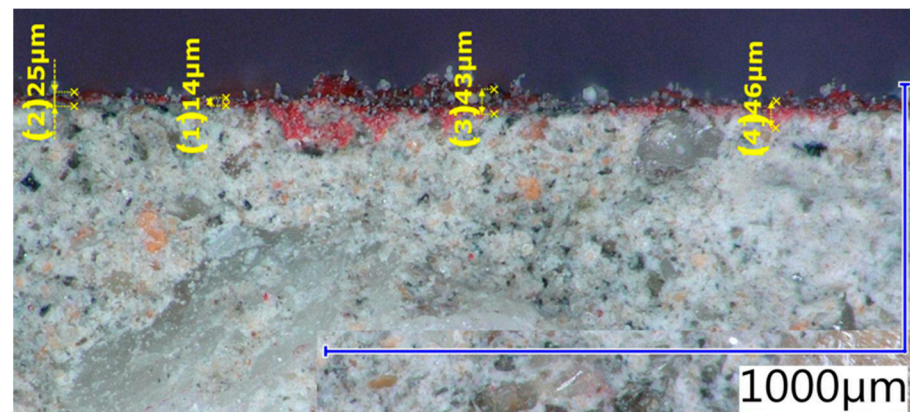
Type of Hydrophobic Impregnation	Viscosity [$\text{mPa}\cdot\text{s}/20\text{ }^{\circ}\text{C}$]	Dilution Ratio
Methylsilanolate base (MS)	40.2	1:0.7 [17]
Silane and siloxane base (SS)	19.7	-
Nano-impregnation (N)	13.0	-

3.2. Penetration Depth

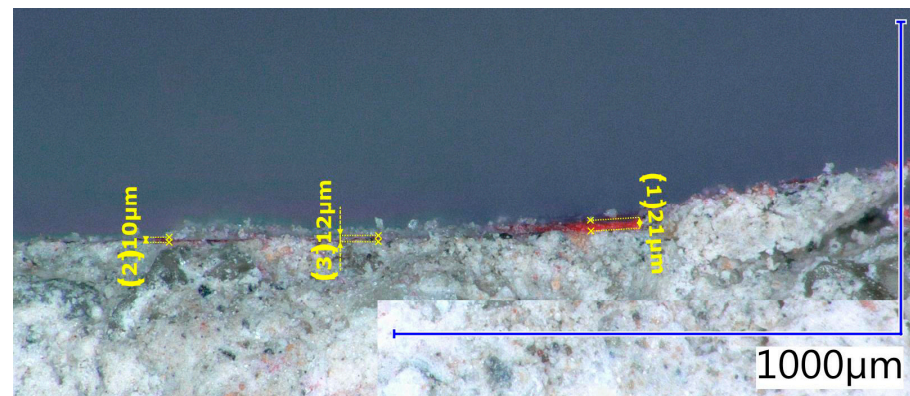
The penetration depth of the hydrophobic MS impregnation applied to S1 ranged from 7 to 25 μm ; see Figure 8a. For S1, treated with hydrophobic N impregnation, the penetration depth ranged from 11–21 μm ; see Figure 8b. For S1, to which the hydrophobic SS impregnation was applied, values of penetration depth between 7 and 46 μm were measured (Figure 8c). From the results, it can be concluded that the depth of penetration is also related to the viscosity of the hydrophobisations. The greatest penetration of the hydrophobisation into the concrete surface was recorded with hydrophobisation based on SS. The depth of penetration of hydrophobisation was also affected by the varied surface of the concrete substrate (distribution of aggregates, cement matrix, pores, etc.).



(a)



(b)



(c)

Figure 8. Depth of penetration of the hydrophobic agents into S1 as determined by digital optical microscope at the magnification of 64×: (a) S1-MS; (b) S1-SS; (c) S1-N.

Basheer et al. [38] reported values ranging from 0.5 to 6.5 mm when measuring the penetration depth of silane or siloxane hydrophobic agents at different concentrations. The penetration depth according to Zhu et al. [6] after the application of a silane-based hydrophobic agent to concrete was also in the range of approximately 2–4 mm. When hydrophobic impregnation was applied by soaking, due to the lower viscosity of the products used, the penetration depth was expected to be higher. The measured results were influenced by the soaking time of the cementitious composite in the hydrophobic impregnation, the drying method and the evaporation ability of the individual components of the hydrophobic impregnations. If some of the components of the hydrophobic agent evaporated too quickly, then the penetration depth could have been adversely affected.

Higher penetration depths could be achieved by soaking the samples several times or by leaving them in the hydrophobic impregnation for longer. These procedures allow the impregnating agent more time to penetrate into the deeper layers of the material.

3.3. Contact Angle

Despite the relatively low penetration depth of the hydrophobic impregnations, all hydrophobic agents increased the substrate's contact angle. For S1, there was an increase in the contact angle of approximately 127% to 130% for all specimens compared with the reference substrate. For S2, 195%, 320% and 210% improvements in contact angle were observed after application of MS, SS and N, respectively.

Graphical evaluation of the results confirming the enhanced hydrophobicity of the S1 and S2 surfaces are shown in Figure 9, where the measured values of contact angles and surface energy changes are shown. It can be seen that the contact angles of the hydrophobically treated samples compared with their untreated substrates increased. The water droplets on reference substrates are shown in Figure 10. The change in the shape of water droplets on substrates treated with hydrophobic impregnations is shown in Figure 11. Based on the results, it can be seen that the application of the hydrophobisations significantly improved the contact angle of the cement composites' surfaces. The surfaces were classified according to the Barnat-Hunek et al. [39] system: hydrophilic (contact angle $< 90^\circ$), hydrophobic (contact angle between 90° and 150°) and superhydrophobic (contact angle $> 150^\circ$). This classification in the graph, together with the data presented, indicates the successful application of hydrophobic impregnations to both substrates.

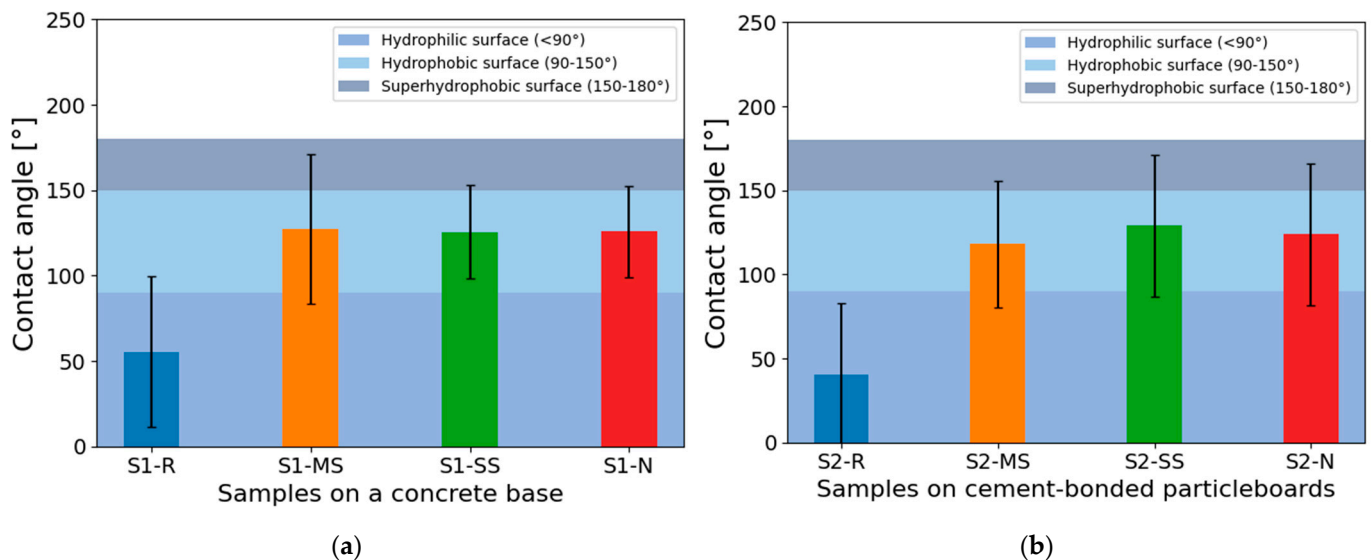


Figure 9. Comparison of water contact angles depending on substrate type: (a) S1; (b) S2.

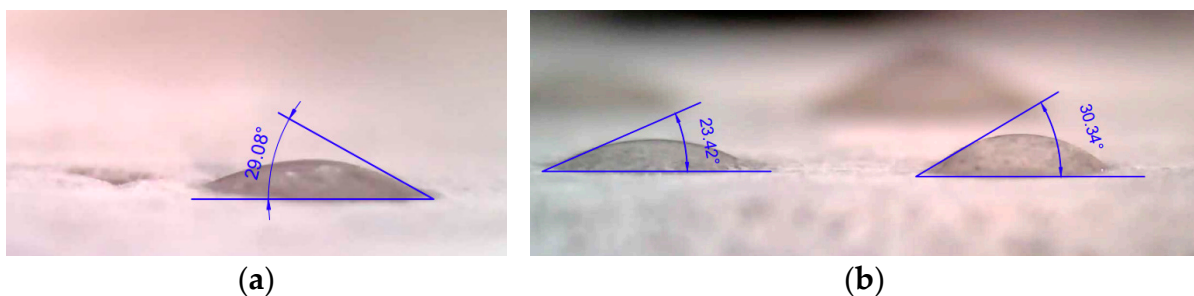


Figure 10. The water droplets on reference substrates: (a) reference substrate S1; (b) reference substrate S2.

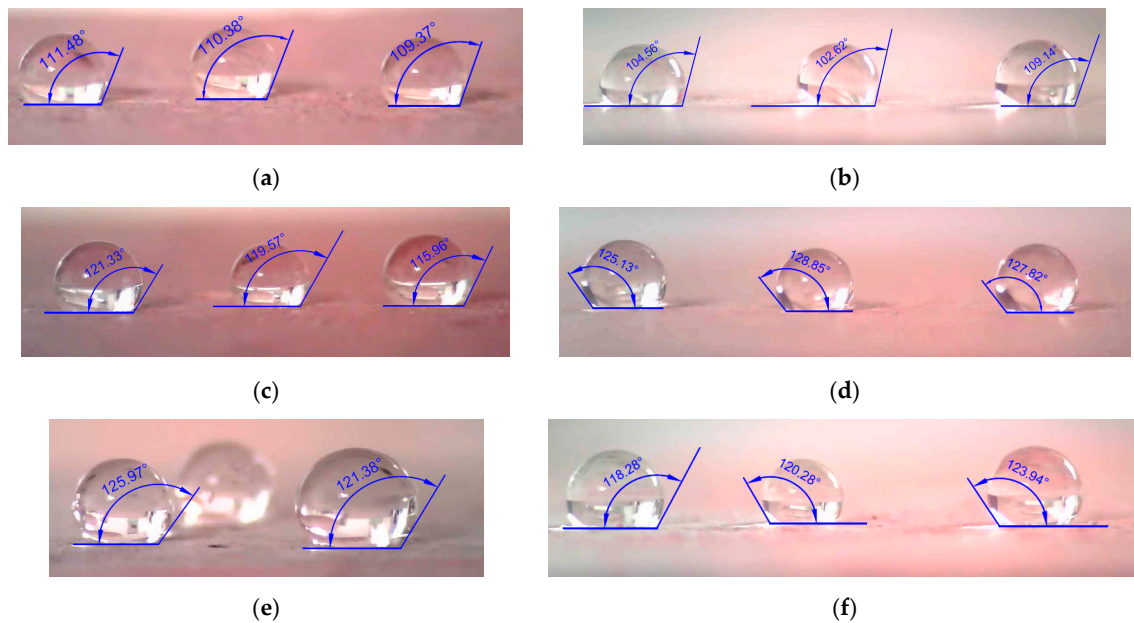


Figure 11. Change in the shape of water droplets on substrates treated with hydrophobic impregnations depending on the type of substrate: (a) S1-MS; (b) S2-MS; (c) S1-SS; (d) S2-SS; (e) S1-N; (f) S2-N.

3.4. Chemical Resistance

The samples after exposure to 10% concentration of CO_2 remained without colour change after the application of the phenolphthalein solution to the fracture surfaces. That is, the pH of all samples was less than 9.0 throughout the sample cross-section. On the samples that were placed in the corrosion SO_2 chamber, it was seen that the pH of the surface layers decreased to a depth of 2–4 mm after the application of the phenolphthalein solution. However, the concrete inside still retained a pH higher than 9.0. For the samples exposed to the aggressive liquid environment of 10% acetic acid, there was a decrease in pH to a depth of 3–4 mm. For the specimens exposed to the 10% sulphuric acid solution, the depth of corrosion ranged from 3 to 6 mm from the surface. Figure 12 shows a comparison of the effect of the aggressive environment on the depth of corrosion for the reference samples and the samples treated with different water-soluble hydrophobisations. The colour change results of the phenolphthalein test after exposure to the samples in the SO_2 atmosphere are shown in Figure 13. The effect of the hydrophobisations on the improvement of the resistance of the concrete to aggressive liquid media (10% H_2SO_4 , 10% CH_3COOH) can be seen in Figures 14 and 15, where a decrease in pH was also measured.

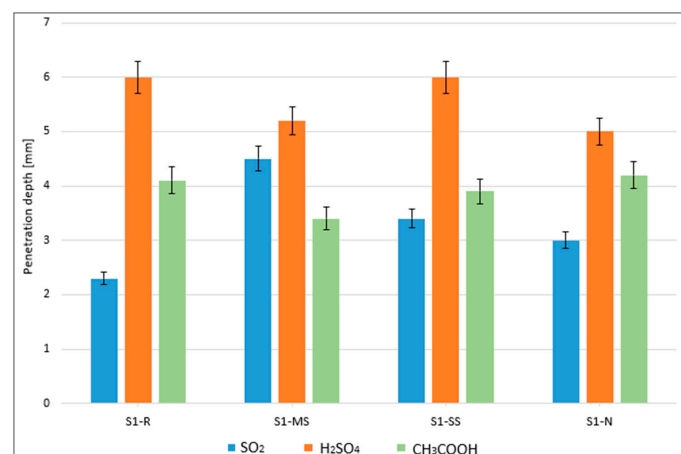


Figure 12. Depth of corrosion of substrate S1 detected by phenolphthalein test.

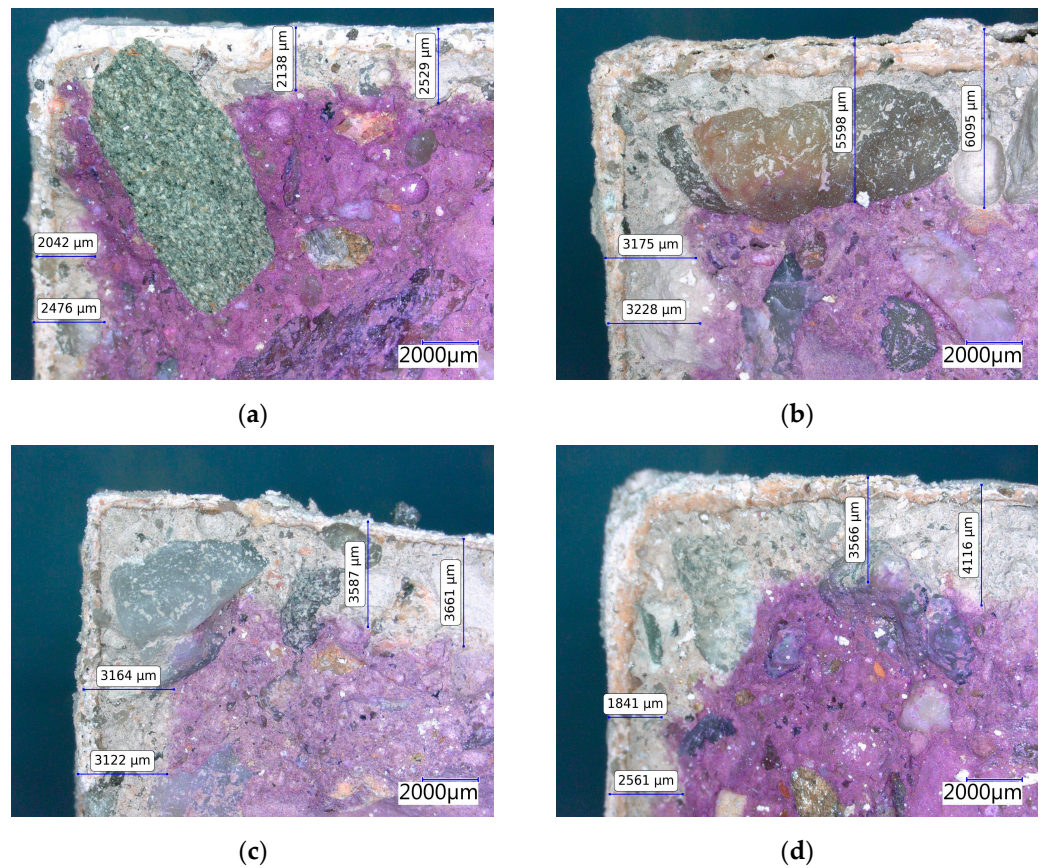


Figure 13. Results of the phenolphthalein test after exposure to the SO_2 atmosphere: untreated reference surface of substrate S1: (a) S1-REF; (b) S1-SM; (c) S1-SS; (d) S1-N.

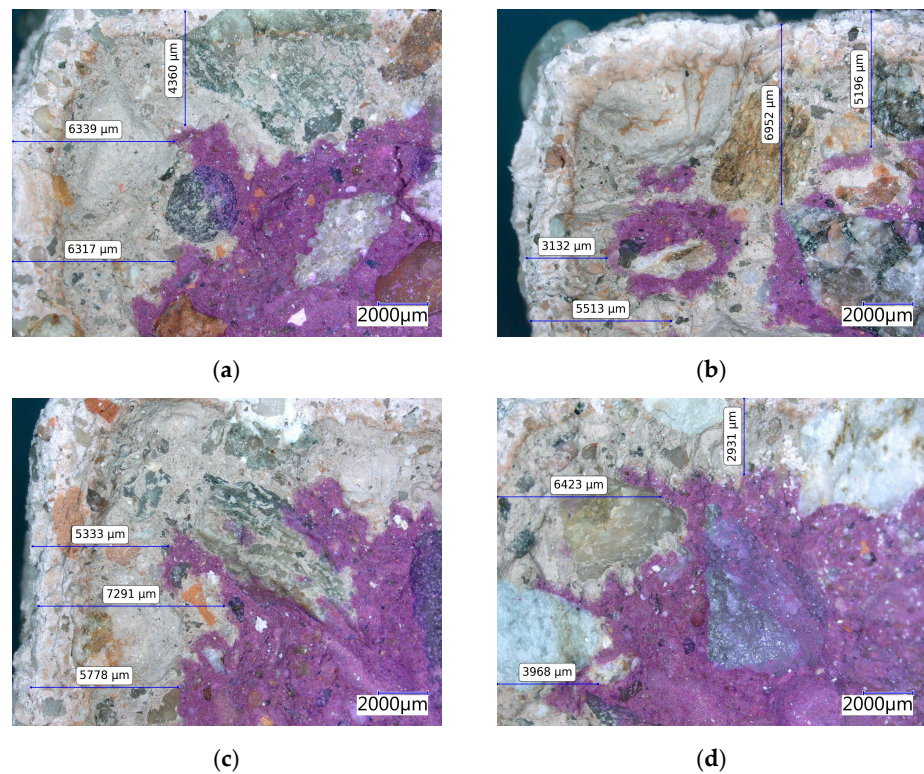


Figure 14. Results of the phenolphthalein test after exposure of samples to 10% H_2SO_4 solution: unmodified reference substrate surface S1 (a); S1-SM (b); S1-SS (c); S1-N (d).

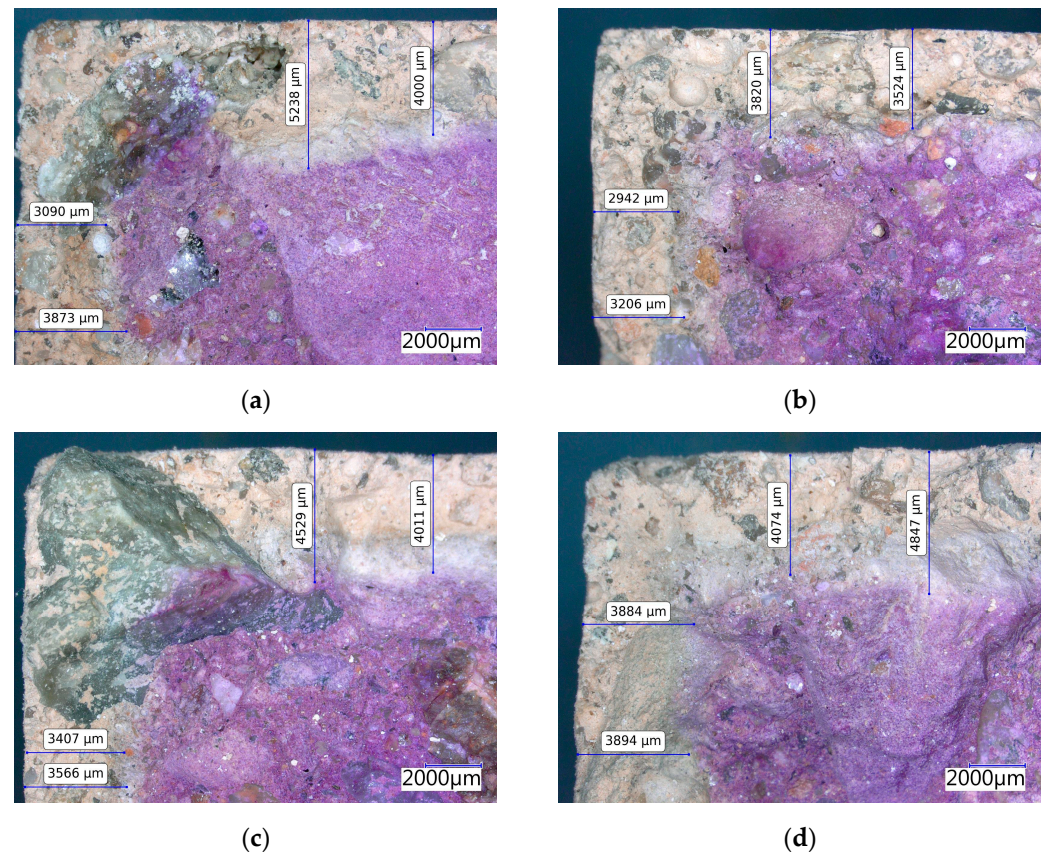


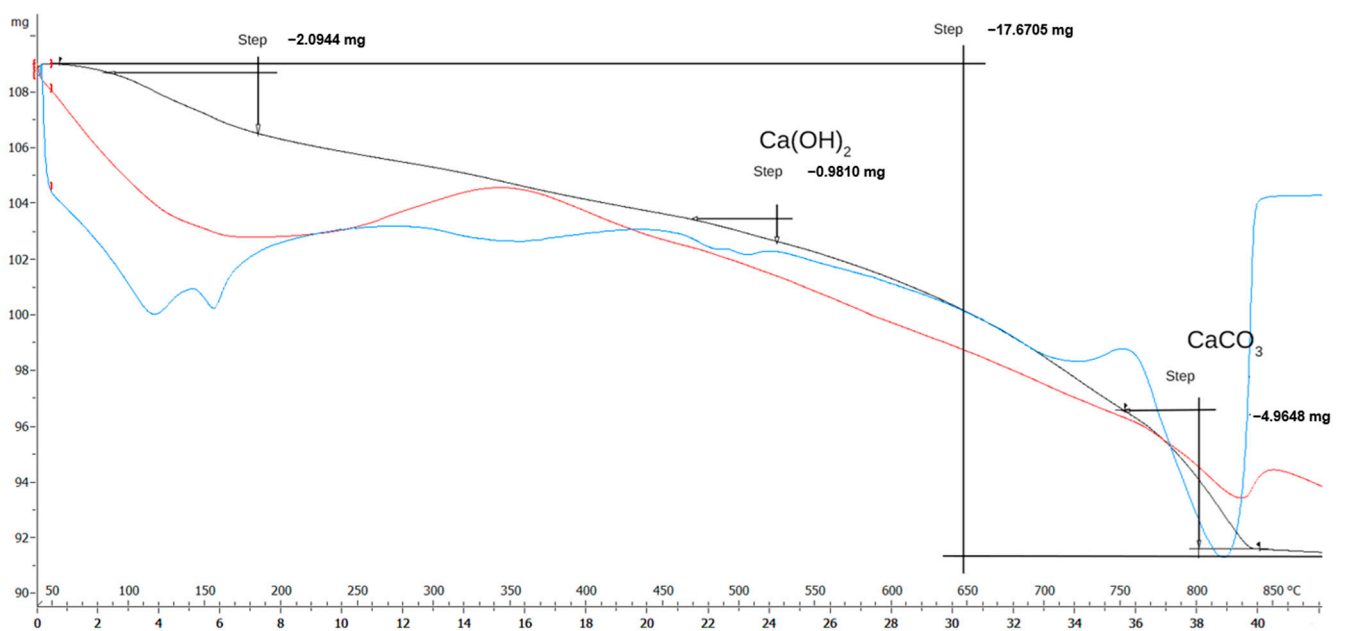
Figure 15. Results of the phenolphthalein test after exposure of samples to 10% CH_3COOH solution: reference substrate surface S1 (a); S1-SM (b); S1-SS (c); S1-N (d).

The CaCO_3 amounts in the S1 samples exposed to conditions accelerating the carbonation process in the CO_2 chamber were 10.36% for the reference sample and 11.34% for the sample treated with the hydrophobic N impregnation. These thermogravimetric results, similar to the study by Chang and Chen [20], indicate changes in $\text{Ca}(\text{OH})_2$ and CaCO_3 contents. As Neville [40] points out in his study on the effects of sulphates on concrete, sulphates react with calcium hydroxide to produce calcium sulphate. In the thermal diffraction analysis of samples exposed to the aggressive gaseous environment with SO_2 , the content of calcium sulphate was determined. For the reference sample, the calcium sulphate concentration was 61.6%. For the sample treated with hydrophobic impregnation, the calcium sulphate concentration was determined to be 67.3%. The mineral content detected by DTA can be seen in Table 6. The output and evaluation of the DTA analysis can be seen in Figure 16a–d. Based on the results of the DTA analysis, it can be concluded that the used hydrophobisation did not positively affect the resistance of concrete to carbonation, as the CaCO_3 content was not lower in the hydrophobised sample (S1-N). In the same way, a higher resistance of hydrophobised concrete to sulfation was not observed; $\text{CaSO}_4 \cdot 2\text{H}_2\text{O}$ content was even lower in the reference sample. The results show that it is necessary to focus more on the method of application of water-soluble hydrophobisations, so that lower amounts of aggressive gases penetrate into the concrete. The microstructure of the S1 samples and the products of carbonation and sulphation are visible in Figures 17 and 18. In the SEM photomicrographs of samples exposed to 10% CO_2 concentration, C-S-H gels, one of the hydration products of cement, can be seen in all samples. The samples exposed to 3.375% SO_2 showed changed microstructures and surface staining, which was also visible without any magnification. When observed using SEM, mineral structures were observed that were similar to ettringite (Figure 17a) and gypsum (Figure 17b,c), which may have been formed by reactions of SO_2 with portlandite or C_3A . Ettringite was mainly observed in the reference sample, where its formation was probably higher, since the concrete was

not surface-treated in any way. In the hydrophobised concrete samples exposed to CO_2 , aragonite (Figure 18c,d) was clearly observable, which was formed as a result of the reaction of portlandite with CO_2 .

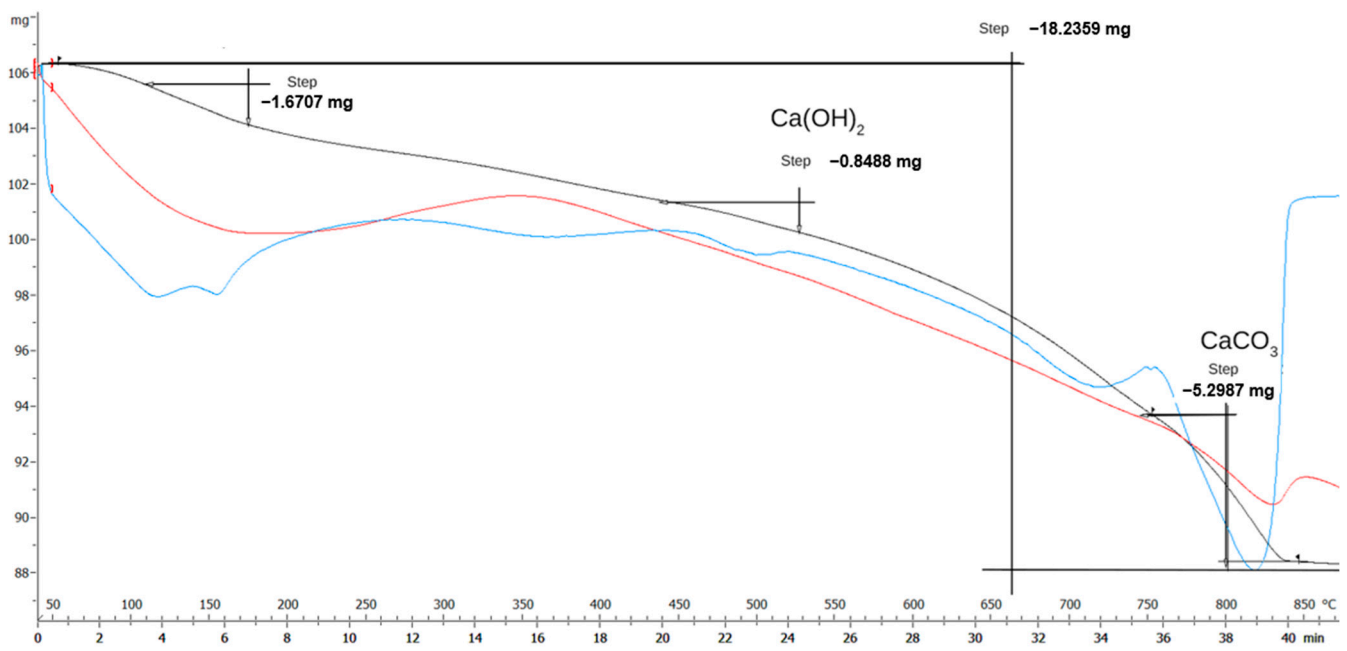
Table 6. Mineral content detected by the DTA analysis.

Sample	Aggressive Environment	Mineral	Content [%]
S1-REF	CO_2	$\text{CaSO}_4 \cdot 2\text{H}_2\text{O}$	-
		$\text{Ca}(\text{OH})_2$	3.70
		CaCO_3	10.36
S1-N	CO_2	$\text{CaSO}_4 \cdot 2\text{H}_2\text{O}$	-
		$\text{Ca}(\text{OH})_2$	3.29
		CaCO_3	11.34
S1-REF	SO_2	$\text{CaSO}_4 \cdot 2\text{H}_2\text{O}$	61.55
		$\text{Ca}(\text{OH})_2$	1.16
		CaCO_3	5.37
S1-N	SO_2	$\text{CaSO}_4 \cdot 2\text{H}_2\text{O}$	67.27
		$\text{Ca}(\text{OH})_2$	1.03
		CaCO_3	5.15

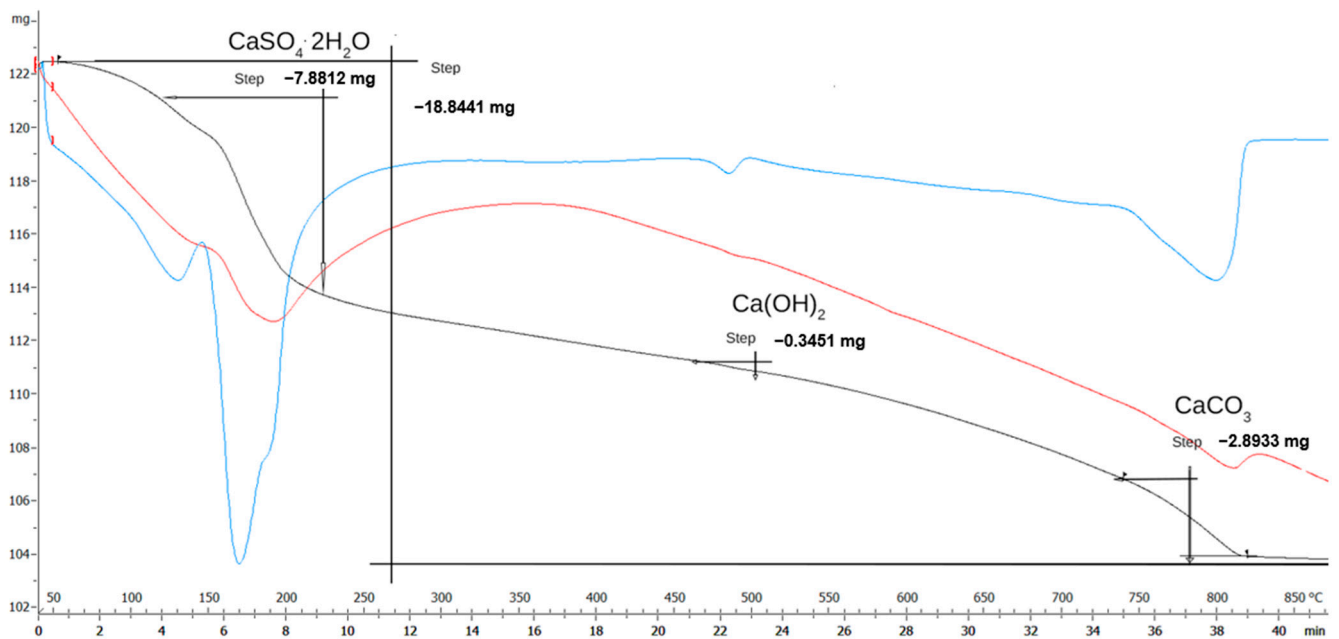


(a)

Figure 16. Cont.

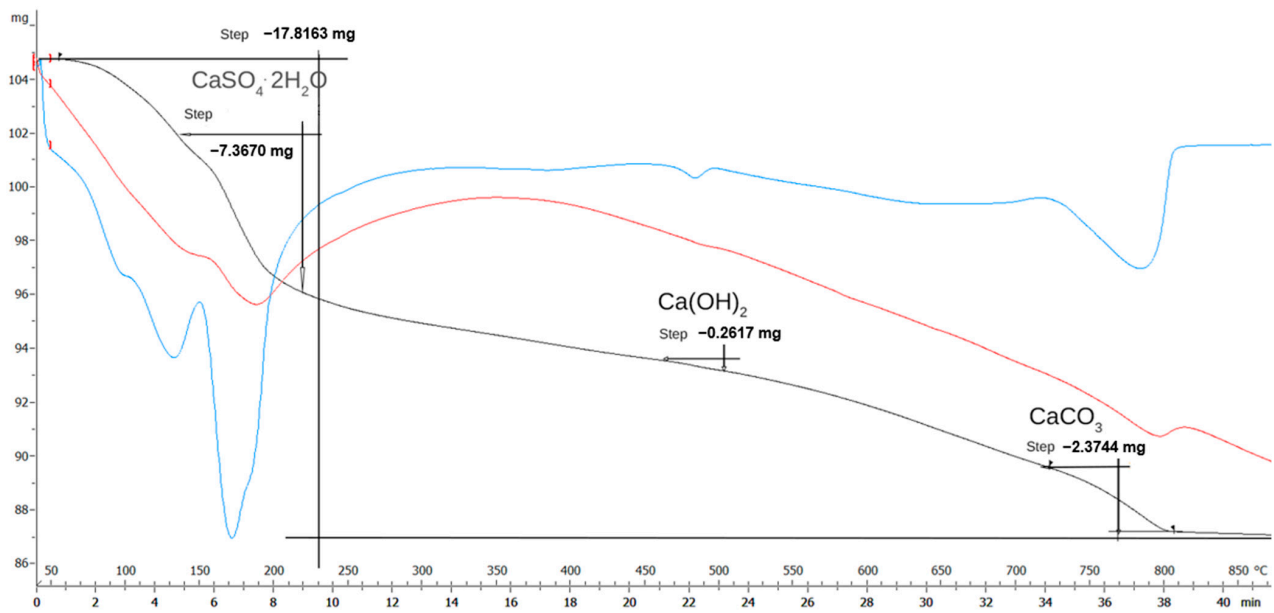


(b)



(c)

Figure 16. Cont.



(d)

Figure 16. Results of DTA analysis after exposure to the CO_2 and SO_2 atmospheres: reference surface of substrate S1 and surface-treated by hydrophobic N impregnation: (a) CO_2 -REF; (b) CO_2 -N; (c) SO_2 -REF; (d) SO_2 -N. (black curve—thermogravimetric (TG) curve, red curve—first derivative of DTA curve, blue curve—DTA curve).

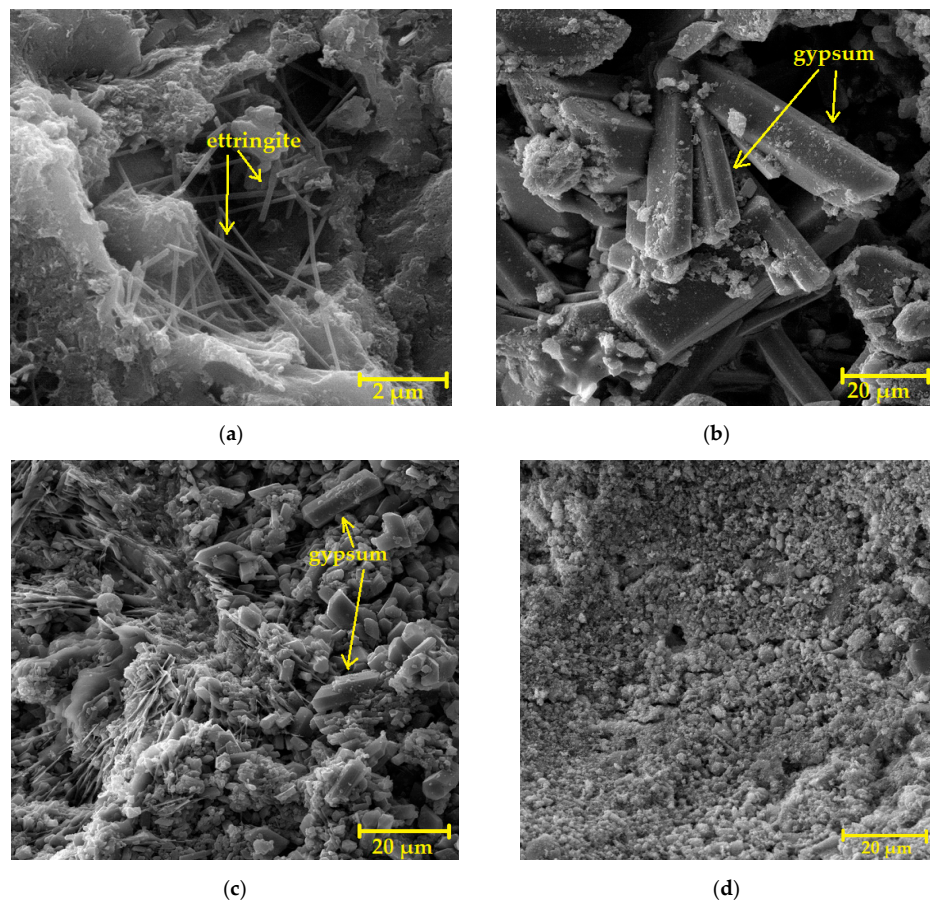


Figure 17. SEM photomicrographs of the surface of samples exposed to the 3.375% SO_2 : (a) S1 without hydrophobic impregnation; (b) S1-MS; (c) S1-SS; (d) S1-N.

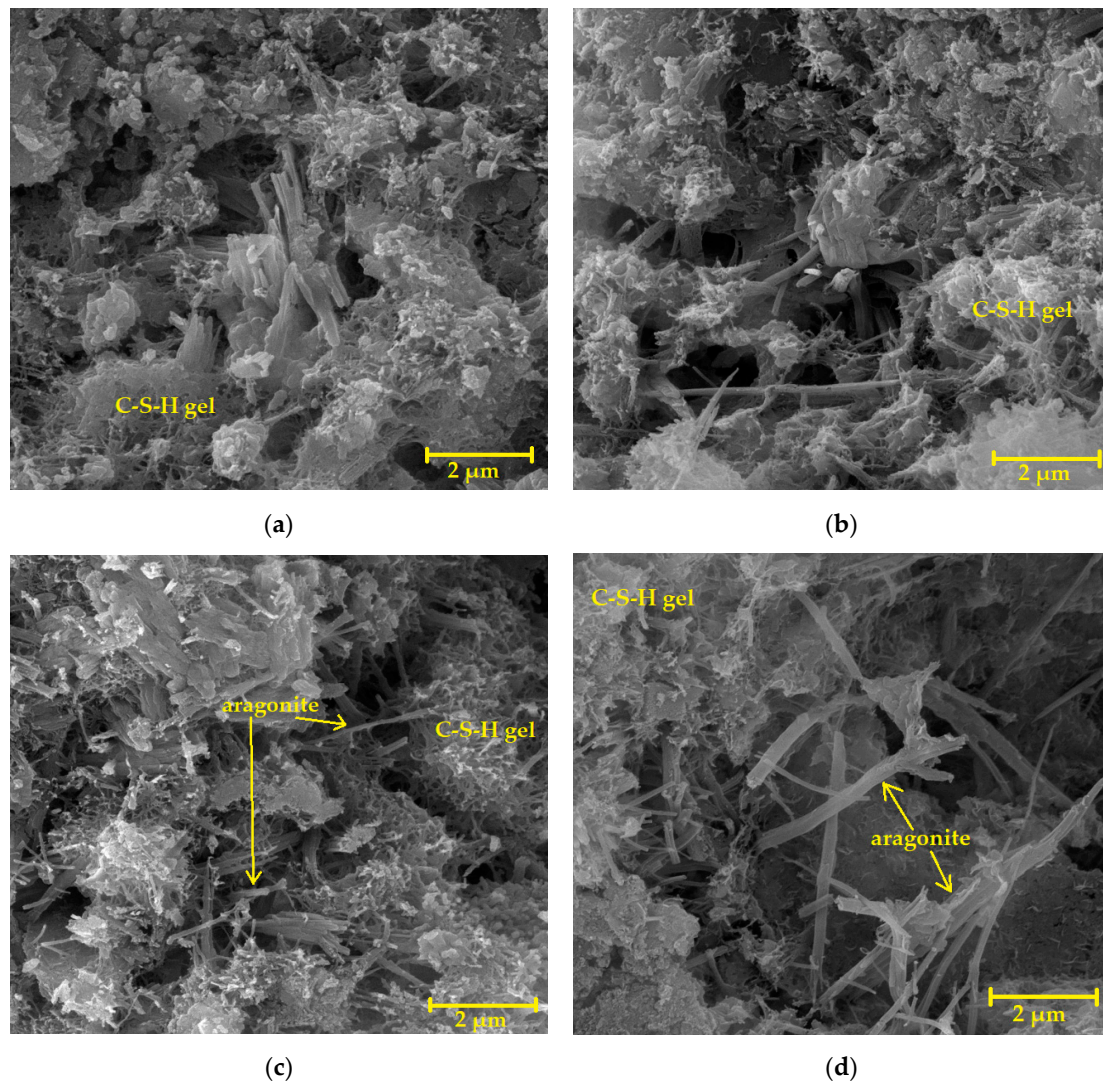


Figure 18. SEM photomicrographs of the surface of samples exposed to 10% CO₂ concentration by SEM (20 kx): (a) S1 without hydrophobic impregnation; (b) S1-MS; (c) S1-SS; (d) S1-N.

3.5. Depth of Penetration of Water Under Pressure

The application of N hydrophobisation reduced the depth of water penetration by 7%. The reduction in penetration depth in samples treated with SS was 16%. However, the use of hydrophobic MS impregnation did not lead to significant improvement. The hydrophobic N and SS impregnations led to a slight reduction in the depth of water pressure penetration, confirming their positive effect on the resistance of cementitious composites to water under pressure [41]. The specimens with measured depths of water pressure penetration are shown in Figure 19. The figure also shows the shapes and widths of seepages, which are very similar for all samples. The average measured values of water penetration into the concrete are shown in Table 7.

Table 7. The maximum depth of water pressure penetration into S1.

Sample	Water Penetration [mm]
S1-R	55
S1-MS	57
S1-SS	46
S1-N	53

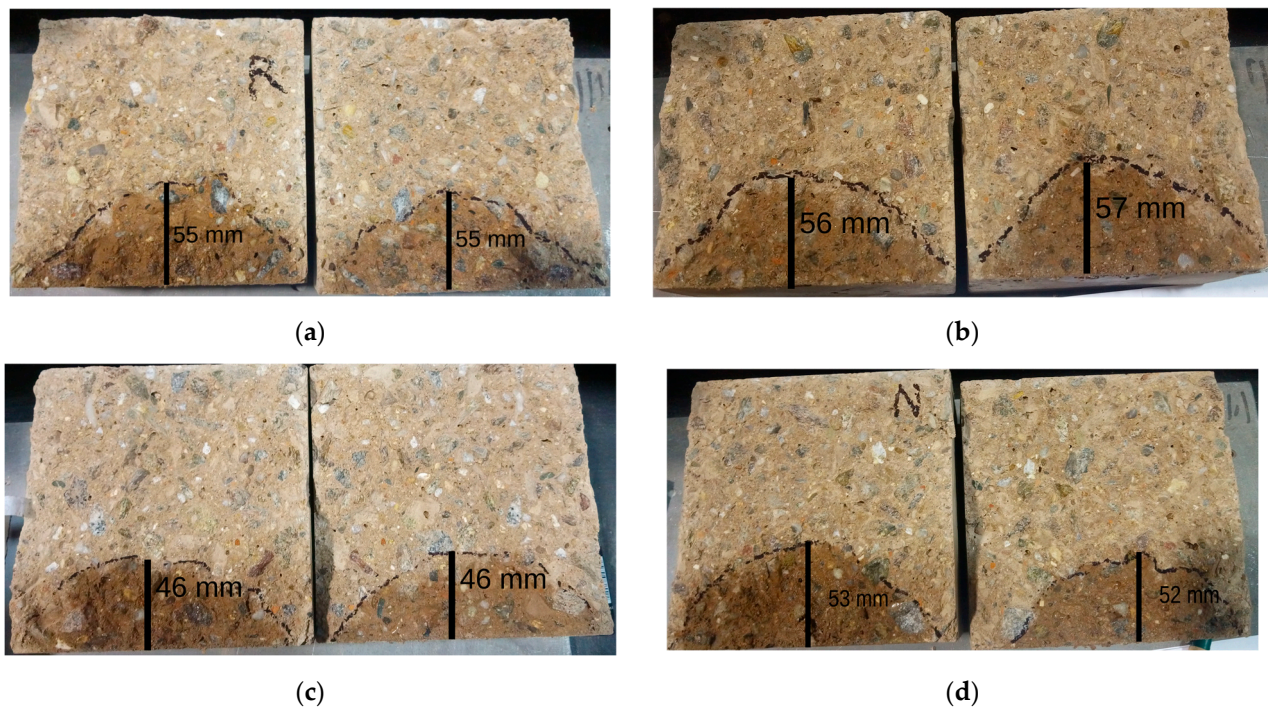


Figure 19. The depth, shape, and width of the pressure water seepage on substrate S1: (a) S1-REF; (b) S1-MS; (c) S1-SS; (d) S1-N.

3.6. Shrinkage

The effect of the application of hydrophobisation on the shrinkage of concrete S1 can be observed immediately after application, as well as at the end of drying and autogenous shrinkage. The application of hydrophobisation shifted the plastic shrinkage phase of concrete samples by a few hours. According to the measured values, the ability of hydrophobisation to modify volume changes of the concrete has the potential to influence the cement composite mechanically and physically. The first 24 h from the beginning of the measurement, when the hydrophobic impregnation was applied, can be seen in Figure 20. Like in Liu et al.'s [42] research, a slight reduction in the shrinkage of the cementitious composite was observed after the application of hydrophobisation. Similar results were also observed for MS and SS hydrophobisations 28 days after the samples' preparation.

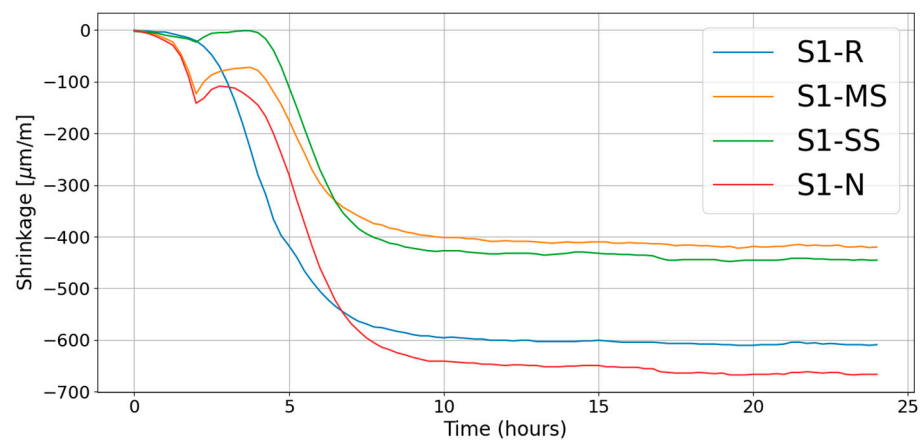


Figure 20. Graphical evaluation of the shrinkage of concrete substrate S1.

3.7. UV Resistance

The first visible change in the S2 specimens was observed after 504 h, when small hairline cracks and slight yellowing appeared on the N-treated S2 specimens. A slight

yellowing of the MS-treated cement-bonded particle board sample also appeared. After 840 h, intense yellowing of the MS-treated specimens could be observed over the entire surface. A yellow colouration could also be observed on the N-treated specimens. In these samples, the staining was not as uniform as in the MS samples but was visible in the form of yellow spots scattered over the surface of the specimens. A similar pattern was also seen on the SS-treated samples, but the stains were less pronounced and were only sporadically present on the surface compared with the N-treated specimens. The samples exposed to 840 cycles and the changes on their surface as well as a comparison with samples stored outside the Q-SUN chamber under laboratory conditions can be seen in Figure 21.

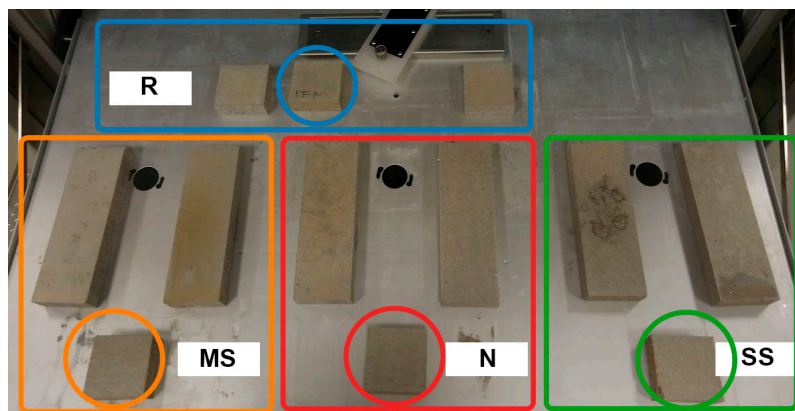


Figure 21. Samples exposed to harsh weather conditions in the Q-SUN chamber after 840 cycles. Samples with the same surface treatment are framed in the same colour. For comparison of visual changes, a sample with the same surface treatment stored under laboratory conditions was attached to the test samples; these are shown in the circles in the figure.

According to Courard et al. [43], UV light exposure destroys Si-O-Si bonds between hydrophobic molecules, and repeated heat cycles can cause irreversible structural changes in the polymer. These changes can lead to the deterioration of the hydrophobic treatment, and this can lead to the visual changes that were observed in this research.

4. Conclusions

The main results of verifying the effect of water-soluble hydrophobic impregnations on the properties of cementitious composites show that:

1. The method of application of the hydrophobic impregnation and the surface properties of the cementitious composites impacted the penetration depth of the hydrophobic impregnation, which is crucial for the effectiveness of the hydrophobic impregnations. Based on the microscopic measurement of the depth of penetration, MS reached an average penetration depth of 14 μm , SS 23 μm and N 15 μm .
2. The application of hydrophobic impregnations significantly increased the contact angle of the surface of cementitious composites (S1, S2). The contact angle was increased in comparison with the reference samples by approximately 2.5 times in the case of all used water-soluble hydrophobisations. The value of the contact angle measured on the concrete substrate S1 was the highest for the MS hydrophobisation used, which was 127.54 degrees. For substrate S2, the highest value of contact angle was measured for the SS specimen, which was 129.09 degrees.
3. The hydrophobically treated specimens contained similar amounts of carbonation products as the reference specimens. This suggests that the application of hydrophobic impregnations did not prevent carbonation and may have even promoted carbonate accumulation in environments with a high concentration of CO_2 .
4. An increase in sulphate levels was observed for both the reference and hydrophobically treated samples after exposure to an atmosphere with an SO_2 concentration of 3.375%. This phenomenon indicates that the applied hydrophobic impregnation

did not provide enhanced protection to the cement composites against the corrosive effects of SO₂ gas.

5. In an aggressive liquid environment, it was observed that the depth of corrosion varied between samples treated with hydrophobic impregnation and untreated reference samples. Hydrophobic impregnation provided moderate protection, increasing the material's resistance to the tested aggressive liquid environment.
6. The measurements showed that the hydrophobic impregnations delayed the plastic shrinkage phase of the concrete. This suggests that hydrophobic treatments can significantly improve the durability of concrete by reducing the risk of early shrinkage cracking. This was observed for the specimens treated with hydrophobic impregnation of MS and SS.

The results show that the method of application of the water-soluble hydrophobic impregnation significantly affected the effectiveness of the surface treatment on the properties of cementitious composites. Soaking the specimens could not provide a uniform layer of hydrophobic impregnation, which in turn affected the other properties of the treated surface.

In summary, it can be said that water-soluble hydrophobic impregnations clearly compete with solvent-based hydrophobisations and significantly contribute to the secondary protection of concrete structures. Based on the shrinkage results, it was proved that the water-soluble hydrophobic impregnations were able to limit the evaporation of water during the hydration of the concrete and thereby contributed to the improvement of its quality. Nowadays and also in the future, water-soluble hydrophobic impregnations are an exclusive option because diluting with water reduces financial costs, and water-soluble hydrophobisations can be chosen from many products on the market based on different binders. Water-soluble hydrophobisations are developed and used in accordance with the environment. Water-soluble hydrophobisations reduce the tendency for staining and “greening” of cement substrates. When drying, they only release water into the environment, as they do not contain any organic solvents.

Author Contributions: Conceptualisation, J.H. and T.B.; methodology, J.H. and R.D.; formal analysis, J.H.; investigation, T.B. and J.H.; resources, J.H. and R.D.; data curation, T.B.; writing—original draft preparation, J.H. and T.B.; writing—review and editing, J.H.; project administration, J.H. and R.D.; funding acquisition, J.H. and R.D. All authors have read and agreed to the published version of the manuscript.

Funding: This research was funded by the financial support of the Czech Science Foundation (GACR), Standard project No. 22-08888S “Increasing the durability of cement composites using water-based hydrophobization”.

Data Availability Statement: Data are contained within the article.

Conflicts of Interest: The authors declare no conflict of interest.

References

1. González-Coneo, J.; Zarzuela, R.; Elhaddad, F.; Carrascosa, L.M.; Gil, M.L.A.; Mosquera, M.J. Alkylsiloxane/alkoxysilane sols as hydrophobic treatments for concrete: A comparative study of bulk vs surface application. *J. Build. Eng.* **2022**, *46*, 103729. [[CrossRef](#)]
2. Sánchez, M.; Faria, P.; Ferrara, L.; Horszczaruk, E.; Jonkers, H.M.; Kwiecień, A.; Mosa, J.; Peled, A.; Pereira, A.S.; Snoeck, D.; et al. External treatments for the preventive repair of existing constructions: A review. *Constr. Build. Mater.* **2018**, *193*, 578–590. [[CrossRef](#)]
3. Zhang, B.; Li, Q.; Ma, R.; Niu, X.; Yang, L.; Hu, Y.; Zhang, J. The Influence of a Novel Hydrophobic Agent on the Internal Defect and Multi-Scale Pore Structure of Concrete. *Materials* **2021**, *14*, 609. [[CrossRef](#)] [[PubMed](#)]
4. Zhang, P.; Li, P.; Fan, H.; Shang, H.; Guo, S.; Zhao, T. Carbonation of Water Repellent-Treated Concrete. *Adv. Mater. Sci. Eng.* **2017**, *2017*, 1343947. [[CrossRef](#)]
5. Courard, L.; Zhao, Z.; Michel, F. Influence of hydrophobic product nature and concentration on carbonation resistance of cultural heritage concrete buildings. *Cement Concr. Compos.* **2021**, *115*, 103860. [[CrossRef](#)]
6. Zhu, Y.-G.; Kou, S.-C.; Poon, C.-S.; Dai, J.-G.; Li, Q.-Y. Influence of silane-based water repellent on the durability properties of recycled aggregate concrete. *Cement Concr. Compos.* **2013**, *35*, 32–38. [[CrossRef](#)]

7. Ebert, D.; Bhushan, B. Wear-resistant rose petal-effect surfaces with superhydrophobicity and high droplet adhesion using hydrophobic and hydrophilic nanoparticles. *J. Colloid Interface Sci.* **2012**, *384*, 182–188. [[CrossRef](#)]
8. Soulios, V.; de Place Hansen, E.J.; Feng, C.; Janssen, H. Hygric behavior of hydrophobized brick and mortar samples. *Build. Environ.* **2020**, *176*, 106843. [[CrossRef](#)]
9. Özek, H.Z. *7-Silicone-Based Water Repellents In The Textile Institute Book Series, Waterproof and Water Repellent Textiles and Clothing*; Williams, J., Ed.; Woodhead Publishing: Cambridge, UK, 2018; pp. 153–189. ISBN 9780081012123.
10. Katsoulis, D.E.; Schmidt, R.G.; Zank, G.A. Chapter 7-Siloxanes and Silicones (Advances in Silicone Technologies 2000–2015). In *Organosilicon Compounds*; Lee, V.Y., Ed.; Academic Press: Cambridge, MA, USA, 2017; pp. 301–322. ISBN 9780128142134.
11. Matziaris, K.; Stefanidou, M.; Karagiannis, G. Impregnation and superhydrophobicity of coated porous low-fired clay building materials. *Prog. Org. Coat.* **2011**, *72*, 181–192. [[CrossRef](#)]
12. Pan, X.; Shi, Z.; Shi, Z.; Shi, C.; Ling, T.; Li, N. A review on concrete surface treatment Part I: Types and mechanisms. *Constr. Build. Mater.* **2017**, *132*, 578–590. [[CrossRef](#)]
13. Buczkowska, K. Hydrophobic protection for building materials. In *Superhydrophobic Coating—Recent Advances in Theory and Applications*; Ou, J., Ed.; Intechopen: London, UK, 2023.
14. Dai, J.G.; Akira, Y.; Wittmann, F.H.; Yokota, H.; Peng, Z. Water repellent surface impregnation for extension of service life of reinforced concrete structures in marine environments: The role of cracks. *Cem. Concr. Compos.* **2010**, *32*, 101–109. [[CrossRef](#)]
15. Kang, S.; Yuan, X.; Liu, C.; Chen, Y.; Zhou, X.; Wu, H.; Ma, Z. Exploration of waterproofness of concrete and alkali-aggregate using hydrophobic impregnation and coating. *J. Renew. Mater.* **2022**, *10*, 3521–3538. [[CrossRef](#)]
16. Zhang, P.; Shang, H.; Hou, D.; Guo, S.; Zhao, T. The effect of water repellent surface impregnation on durability of cement-based materials. *Adv. Mater. Sci. Eng.* **2017**, *2017*, 8260103. [[CrossRef](#)]
17. Herb, H.; Gerdes, A.; Brenner-Weiß, G. Characterization of silane-based hydrophobic admixtures in concrete using TOF-MS. *Cem. Concr. Res.* **2015**, *70*, 77–82. [[CrossRef](#)]
18. Wu, Y.; Dong, L.; Shu, X.; Yang, Y.; She, W.; Ran, Q. A review on recent advances in the fabrication and evaluation of superhydrophobic concrete. *Compos. B Eng.* **2022**, *237*, 109867. [[CrossRef](#)]
19. Gao, D.; Yang, L.; Pang, Y.; Li, Z.; Tang, Q. Effects of a novel hydrophobic admixture on the sulfate attack resistance of the mortar in the wet-dry cycling environment. *Constr. Build. Mater.* **2022**, *344*, 128148. [[CrossRef](#)]
20. Jiang, L.; Xue, X.; Zhang, W.; Yang, J.; Zhang, H.; Li, Y.; Zhang, R.; Zhang, Z.; Xu, L.; Qu, J.; et al. The investigation of factors affecting the water impermeability of inorganic sodium silicate-based concrete sealers. *Constr. Build. Mater.* **2015**, *93*, 729–736. [[CrossRef](#)]
21. Szymańska, A.; Dutkiewicz, M.; Maciejewski, H.; Palacz, M. Simple and effective hydrophobic impregnation of concrete with functionalized polybutadienes. *Constr. Build. Mater.* **2022**, *315*, 125624. [[CrossRef](#)]
22. Perko, J.; Zarzuela, R.; Garcia-Lodeiro, I.; Blanco-Varela, M.T.; Mosquera, M.J.; Seemann, T.; Yu, L. The importance of physical parameters for the penetration depth of impregnation products into cementitious materials: Modelling and experimental study. *Constr. Build. Mater.* **2020**, *257*, 119595. [[CrossRef](#)]
23. Meier, S.J.; Wittmann, F.H. Recommendations for water repellent surface impregnation of concrete. *Restor. Build. Monum.* **2011**, *17*, 347–358. [[CrossRef](#)]
24. Behravan, A.; Aqib, S.M.; Delatte, N.J.; Ley, M.T.; Rywelski, A. Performance evaluation of silane in concrete bridge decks using transmission X-ray microscopy. *Appl. Sci.* **2022**, *12*, 2557. [[CrossRef](#)]
25. Al-Kheetan, M.J.; Rahman, M.M.; Chamberlain, D.A. Moisture evaluation of concrete pavement treated with hydrophobic surface impregnants. *Int. J. Pavement Eng.* **2020**, *21*, 1746–1754. [[CrossRef](#)]
26. Sohawon, H.; Beushausen, H. The effect of hydrophobic (silane) treatment on concrete durability characteristics. *MATEC Web Conf.* **2018**, *199*, 07015. [[CrossRef](#)]
27. *Technical Data Sheet of Silicone Water-Soluble Hydrophobizing Agent LUKOFOB 39*; Lučební závody a.s. Kolín: Kolín, Czech Republic, 2017.
28. NanoConcept®. In *Technical Data Sheet of Nanoimpregnation of Concrete NanoConcept®*; IMPRE CZ s.r.o: Brno, Czech Republic, 2021.
29. *Technical Data Sheet 360 of Preservative Impregnation against Weathering PCI Silconal® W*; PCI Augsburg GmbH: Augsburg, Germany, 2021.
30. CETRIS®. In *Technical Data Sheet of Cement-Bonded Particleboard CETRIS® BASIC*; CIDEM Hranice a.s.: Hranice, Czech Republic.
31. *EN 1328*; Cement Bonded Particleboards—Determination of Frost Resistance. European Committee for Standardization (CEN): Brussels, Belgium; Technical Committee CEN/TC112/WG6: Geneva, Switzerland, 1998.
32. *ČSN 73 1326*; Determination of the Resistance of the Surface of Cement Concrete against the Action of Water and Chemical Deicers. Czech Standardization Institute (CSI): Prague, Czech Republic, 1985.
33. *EN ISO 2884-2*; Paints and Varnishes—Determination of Viscosity Using Rotary Viscometers—Part 2: Disc or Ball Viscometer Operated at a Specified Speed. European Committee for Standardization (CEN): Brussels, Belgium; Technical Committee ISO/TC35/SC9: Geneva, Switzerland, 2003.
34. *EN ISO 22479*; Corrosion of Metals and Alloys—Sulfur Dioxide Test in a Humid Atmosphere (Fixed Gas Method). European Committee for Standardization (CEN): Brussels, Belgium; Technical Committee ISO/TC156: Geneva, Switzerland, 2019.
35. Ashraf, W. Carbonation of cement-based materials: Challenges and opportunities. *Constr. Build. Mater.* **2016**, *120*, 558–570. [[CrossRef](#)]

36. EN 12390; Testing Hardened Concrete—Part 8: Depth of Penetration of Water under Pressure. European Committee for Standardization (CEN): Brussels, Belgium; Technical Committee CEN/TC104/SC1: Geneva, Switzerland, 2019.
37. EN ISO 4892-2; Plastics—Methods of Exposure to Laboratory Light Sources, Part 2: Xenon-Arc Lamps. European Committee for Standardization (CEN): Brussels, Belgium; Technical Committee ISO/TC61/SC6: Geneva, Switzerland, 2013.
38. Basheer, L.; Cleland, D.J.; Long, A.E. Protection provided by surface treatments against chloride induced corrosion. *Mater. Struct.* **1998**, *31*, 459–464. [[CrossRef](#)]
39. Barnat-Hunek, D.; Grzegorzczak-Frańczak, M.; Suchorab, Z. Surface hydrophobisation of mortars with waste aggregate by nanopolymer triethoxy-isobutyl-silane and methyl silicon resin. *Constr. Build. Mater.* **2020**, *264*, 120175. [[CrossRef](#)]
40. Neville, A. The confused world of sulfate attack on concrete. *Cem. Concr. Res.* **2004**, *34*, 1275–1296. [[CrossRef](#)]
41. Santos, W.F.; Quattrone, M.; John, V.M.; Angulo, S.C. Roughness, wettability and water absorption of water repellent treated recycled aggregates. *Constr. Build. Mater.* **2017**, *146*, 502–513. [[CrossRef](#)]
42. Liu, X.; Song, X.; Wang, Z.; Xia, C.; Li, T.; Li, X.; Xu, Q.; Cui, S.; Qian, S. Polymer for internal hydrophobization of cement-based materials: Design, synthesis, and properties. *Polymers* **2021**, *13*, 3069. [[CrossRef](#)]
43. Courard, L.; Vincent, L.; Olivier, G.; Myriam, H.; Michel, F.; Aggoun, S.; Cousture, A. Evaluation of the Durability of Hydrophobic Treatments on Concrete Architectural Heritage. In *Hydrophobe VII, 7th International Conference on Water Repellent Treatment and Protective Surface Technology for Building Materials*; Charola, A.E., Delgado Rodrigues, J., Eds.; LNEC: Lisbon, Portugal; Smithsonian: Washington, DC, USA, 2014; pp. 29–38.

Disclaimer/Publisher’s Note: The statements, opinions and data contained in all publications are solely those of the individual author(s) and contributor(s) and not of MDPI and/or the editor(s). MDPI and/or the editor(s) disclaim responsibility for any injury to people or property resulting from any ideas, methods, instructions or products referred to in the content.